Mechanisms of chromosome number reduction in *Arabidopsis thaliana* and related Brassicaceae species

Martin A. Lysak*†, Alexandre Berr‡, Ales Pecinka‡, Renate Schmidt§, Kim McBreen¶, and Ingo Schubert‡

*Jodrell Laboratory, Royal Botanic Gardens, Kew, Richmond TW9 3AB, United Kingdom; ‡Leibniz-Institute of Plant Genetics and Crop Plant Research (IPK), Corrensstrasse 3, 06466 Gatersleben, Germany; §Max-Planck-Institut für Molekulare Pflanzenphysiologie, 14424 Potsdam, Germany; and ¶Allan Wilson Centre for Molecular Ecology and Evolution, Massey University, Palmerston North, New Zealand

Edited by Maarten Koornneef, Wageningen University and Research Centre, Wageningen, The Netherlands, and approved February 1, 2006 (received for review December 14, 2005)

Evolution of chromosome complements can be resolved by genome sequencing, comparative genetic mapping, and comparative chromosome painting. Previously, comparison of genetic maps and gene-based phylogenies suggested that the karyotypes of *Arabidopsis thaliana* ($n = 5$) and of related species with six or seven chromosome pairs were derived from an ancestral karyotype with eight chromosome pairs. To test this hypothesis, we applied multicolor chromosome painting using contiguous bacterial artificial chromosome pools of *A. thaliana* arranged according to the genetic maps of *Arabidopsis lyrata* and *Capsella rubella* (both $n = 8$) to *A. thaliana*, *A. lyrata*, *Neslia paniculata*, *Turritis glabra*, and *Hornungia alpina*. This approach allowed us to map the *A. lyrata* centromeres as a prerequisite to defining a putative ancestral karyotype ($n = 8$) and to elucidate the evolutionary mechanisms that shaped the karyotype of *A. thaliana* and its relatives. We conclude that chromosome "fusions" in *A. thaliana* resulted from (*i*) generation of acrocentric chromosomes by pericentric inversions, (*ii*) reciprocal translocation between two chromosomes (one or both acrocentric), and (*iii*) elimination of a minichromosome that arose in addition to the "fusion chromosome." Comparative chromosome painting applied to *N. paniculata* ($n = 7$), *T. glabra* ($n = 6$), and *H. alpina* ($n = 6$), for which genetic maps are not available, revealed chromosomal colinearity between all species tested and allowed us to reconstruct the evolution of their chromosomes from a putative ancestral karyotype ($n = 8$). Although involving different ancestral chromosomes, chromosome number reduction followed similar routes as found within the genus *Arabidopsis*.

chromosome painting | genome homeology | karyotype evolution | genome colinearity | phylogeny

The specific chromosome complement of a eukaryotic organism, the karyotype, may vary as to the number, size, and shape of chromosomes even between closely related taxa. Size and/or shape of chromosomes may change by means of reciprocal translocations, inversions, insertions, or deletions. At the diploid level, chromosome numbers may vary because of meiotic missegregation in translocation heterozygotes or by so-called fusion/fission events (1, 2). Such mechanisms combined with doubling of entire complements (polyploidy) have generated the extant karyotypes in the course of evolution. Because karyotypes are dynamic structures, the reconstruction of ancestral karyotypes on the basis of well described extant karyotypes is necessary to understand the evolutionary direction of karyotypic variation. In principle, there are two strategies to uncover putative ancestral karyotypes and to reconstruct the evolutionary events that led to the present karyotypes, both based on comparison of chromosome colinearity shared by extant species. One strategy is comparative genetic mapping, as exemplified for grasses (3); the other is comparative chromosome painting (CCP), successfully applied to vertebrates (for review, see refs. 4 and 5).

Among species of the Brassicaceae family, chromosome numbers vary from $n = 4$ to 128 (6). Within the genus *Arabidopsis* and its close relatives, basic chromosome numbers vary between 5, 6, 7, and 8, with most species having 8 chromosome pairs. Based on comparative genetic maps between *Arabidopsis thaliana* ($n = 5$) and *Arabidopsis lyrata* ($n = 8$; refs. 7 and 8) as well as between *A. thaliana* and *Capsella rubella* ($n = 8$; ref. 9) and on DNA sequence-derived phylogenetic trees (10), an ancestral karyotype with 8 chromosomes has been inferred. It has been suggested that the karyotype of *A. thaliana* descended from the ancestral karyotype by two reciprocal translocations, three chromosome fusions, and at least three inversions (8, 11).

Here, we studied chromosomal colinearity between *A. thaliana* and four cruciferous species with different chromosome numbers (*A. lyrata*, $n = 8$; *Neslia paniculata*, $n = 7$; *Turritis glabra*, $n = 6$; and *Hornungia alpina*, $n = 6$) by CCP with bacterial artificial chromosome (BAC) contigs covering all chromosome arms of *A. thaliana*. The CCP results were compared with the genetic maps in the context of phylogenetic relationships based on multiple gene sequences. For *A. lyrata*, chromosome painting confirmed the pattern of genome colinearity derived from the *A. thaliana*/*A. lyrata* genetic maps (7, 8). Moreover, we present new insights as to the centromere positions within the ancestral karyotype and the role of specific inversion and translocation events during chromosome number reduction from $n = 8$ to $n = 5$ in *A. thaliana*. Applying CCP to the three species with six or seven chromosome pairs for which genetic maps are not available, we uncovered the extent of chromosomal colinearity between these species and *A. thaliana*. We identified events associated with the chromosome number reduction as compared with the ancestral karyotype.

Results

Chromosome Painting Confirmed and Specified the Evolutionary Events Toward the *A. thaliana* Karyotype. To address the chromosomes that correspond to the linkage groups (LGs) of *A. lyrata* (7, 8), multicolor CCP was applied to its pachytene chromosomes. *A. thaliana* BAC contigs arranged according to the eight LGs (Fig. 1*B*) labeled one bivalent each. The position of all centromeres and of the five nucleolus organizing regions (NORs) (on the short arms of chromosomes 1, 3–5, and 7) has been determined for the *A. lyrata* karyotype (Fig. 1 *B* and *D–F*). Because the LGs of *A. lyrata* largely correspond to those of the more distantly related *C. rubella* (11), the karyotypes of both species should be similar to the ancestral karyotype (AK) of the entire *Arabidopsis* lineage.

Conflict of interest statement: No conflicts declared.

This paper was submitted directly (Track II) to the PNAS office.

Abbreviations: BAC, bacterial artificial chromosome; CCP, comparative chromosome painting; LG, linkage group; AT, chromosome of *Arabidopsis thaliana*; AK, ancestral karyotype; NOR, nucleolus organizing region.

Data deposition: The sequences reported in this paper have been deposited in the GenBank database (accession nos. AF167571, M64119, AY198405, X52320, AP000423, and DQ310510–DQ310545).

†To whom correspondence should be addressed at: Jodrell Laboratory, Royal Botanic Gardens, Kew, Richmond, Surrey TW9 3AB, United Kingdom. E-mail: m.lysak@kew.org.

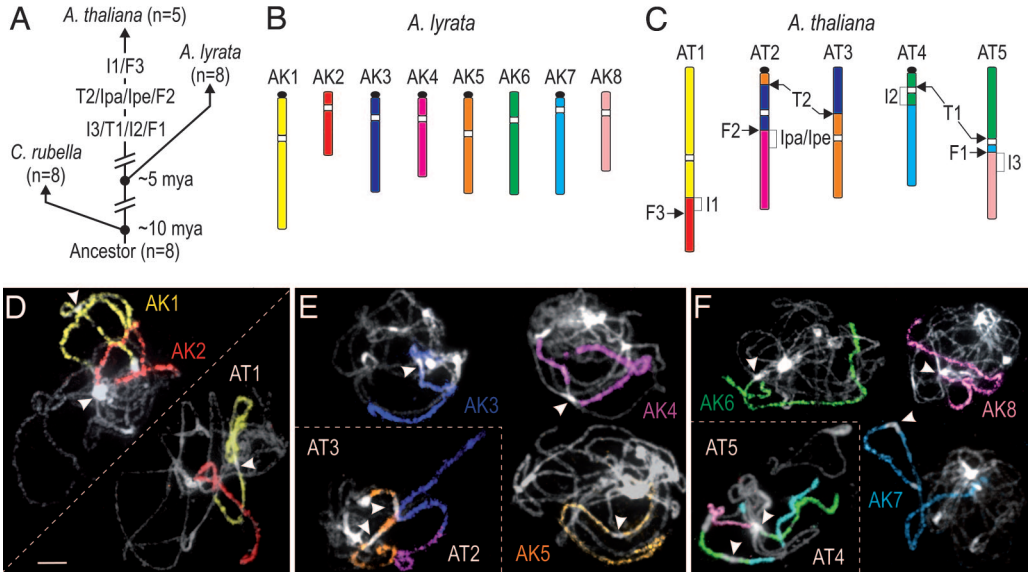

Fig. 1. Evolution of the *A. thaliana* ($n = 5$) karyotype based on comparative chromosome painting in *A. lyrata* ($n = 8$). (*A*) The events leading to chromosome number reduction in the course of evolution from an ancestor with $n = 8$ chromosomes toward the karyotype of *A. thaliana*. Inversion (I), translocation (T), and fusion events (F) as well as divergence time estimates are from Koch and Kiefer (11). Only consecutive paracentric and pericentric inversions (Ipa/Ipe) within AK4 are newly proposed. Events that require a distinct chronological order are arranged together. (*B*) Idiogram of the *A. lyrata* karyotype. The chromosomes correspond to the ancestral karyotype, with the NORs (black spheres) actually found in *A. lyrata*. (*C*) Idiogram of the *A. thaliana* karyotype indicating the composition of chromosomes AT1 to -5 derived from the ancestral karyotype (*B*) and the events involved in chromosome number reduction shown in *A*. (*D–F*) Pachytene chromosomes of *A. thaliana* (AT1 to -5) and *A. lyrata* (AK1 to -8) painted by *A. thaliana* BAC contigs arranged according to the linkage groups of *A. lyrata* and pseudocolored according to *B*; empty squares/arrowheads indicate centromeric regions. (Scale bar: 5 μm in *D–F*.)

With the aim of visualizing the components of the ancestral karyotype with eight chromosome pairs (AK1 to -8) on the five *A. thaliana* chromosomes, multicolor painting was performed with BAC pools arranged according to entire or partial LGs of *A. lyrata* (Figs. 1 *C–F* and 2*A*). Probes painting *A. thaliana* chromosomes 1 (AT1) hybridized also to the two *A. lyrata* chromosomes that correspond to LGs 1 and 2 matching with comparative mapping results. The BAC contig covering the distal part of the bottom arm of AT1 and homeologous to LG2 labeled the entire AK2 chromosome of *A. lyrata* (Fig. 1*D*). Subdividing the probe for LG2 in three differently labeled subcontigs revealed an inversion comprising the top (short) arm of AK2 (Fig. 2*A*). This inversion has been detected by genetic mapping in *C. rubella* (9) and very recently also in *A. lyrata* (12). Because neither centromeric nor telomeric sequences of chromosome AK2 were detected at the point of "fusion" within AT1 (13), we conclude that a pericentric inversion transformed AK2 into an acrocentric chromosome. This inversion event was followed by a reciprocal translocation between the short arm end of AK1 and the centric end of AK2, resulting in AT1 (Fig. 2*B*). The second very small translocation product, consisting mainly of telomeric repeats from AK1 and AK2 and of the AK2 centromere, became lost most likely because it failed to pair properly during meiosis and lacked essential genes.

Probes designed according to *A. lyrata* LGs 3, 4, and 5 labeled chromosomes AT2 and AT3 (Fig. 1*E*). Thus, AT2 comprises the terminal part of the top arm of AK5, followed by the proximal part of the bottom arm, the centromere, and the top (short) arm of AK3 and by the entire AK4 (without a centromere). AT3 is homeologous to the bottom arm, the centromere, and part of the top arm of AK5, and a large part of the bottom arm of AK3 (Fig. 1*C*). Our data show that the centromeres of AT2 and AT3 retained the same position as in AK3 and AK5 and confirm that chromosomes AT2 and AT3 have been formed by a reciprocal translocation between AK3 and AK5, as indicated previously (7, 8, 11). Within AK4, no pericentric inversion involving the top arm was found by FISH with pools subdividing this region. However, a paracentric inversion constituting the entire short arm, followed by a pericentric one, could have generated an acrocentric AK4 that fused with AK3/5 to AT2 by a reciprocal translocation without interrupting colinearity to LG4. The small second translocation product consisting of telomeres and the centromere of AK4 was lost (Fig. 2*C*).

Probes designed according to *A. lyrata* LGs 6, 7, and 8 labeled chromosomes AT4 and AT5 (Fig. 1*F*). AT4 is homeologous to the top (short) arm of AK6 and to the bottom arm of AK7. Chromosome AT5 comprises the bottom (long) arm of AK6, the top (short) arm of AK7, and the entire AK8 (without a centromere). The first step toward the recent chromosomes AT4 and AT5 was a reciprocal translocation apparently between the centromeres of AK6 and AK7 (Fig. 2*D*). The inversion in the long arm of AT4 was originally detected by genetic mapping (8, 9) and could be confirmed by CCP. This apparently pericentric inversion (14) occurred simultaneously with or after the translocation between AK6 and AK7. Another inversion within the bottom arm of AT5 in comparison with *C. rubella* linkage group H (8, 9, 11) originally generated an acrocentric chromosome from AK8. Finally, a reciprocal translocation "fused" this acrocentric with AK6/7 to AT5 (Fig. 2*D*). Thus, this fusion followed the same scheme as the fusion that contributed to the formation of AT1 (Fig. 2*B*).

CCP Reveals the Modes of Chromosome Number Reduction also for Species Lacking Genetic Maps. To elucidate the karyotype evolution from the putative ancestral karyotype toward the karyotypes of *N. paniculata*, *T. glabra*, and *H. alpina* (all $n < 8$), BAC pools arranged according to the eight LGs (or particular regions thereof) of *A. lyrata*/*C. rubella* were used for CCP.

Fig. 3*A1* shows the reconstructed karyotype of *N. paniculata* ($n = 7$). Probes designed according to the reference LGs 1–3 and 6–8 each labeled an individual pachytene bivalent or mitotic chromosome pair (Fig. 3 *A3–A5*). CCP with the probe corre-

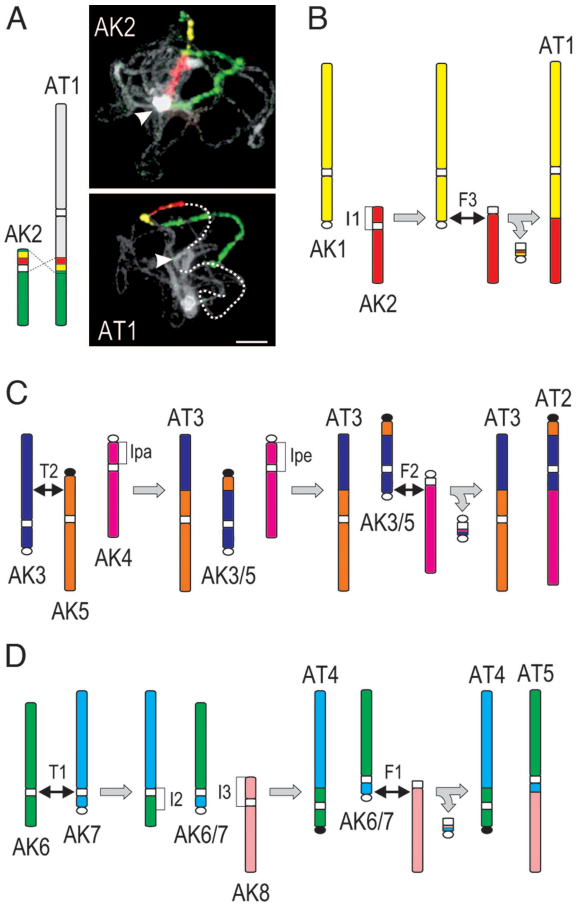

Fig. 2. Reconstruction of *A. thaliana* fusion chromosomes. (*A*) Painting of AK2 chromosome of *A. lyrata* and AT1 chromosome of *A. thaliana* with differently labeled BAC pools covering LG 2 of *A. lyrata* shows that a pericentric inversion has occurred before AK2 became fused with AK1 during the evolution toward *A. thaliana*. Empty squares/arrowheads indicate centromeric regions. (Scale bar: 5 μm.) (*B*) The origin of fusion chromosome AT1 by a pericentromeric inversion within AK2 followed by a reciprocal translocation with breakpoints at the short arm end of AK1 and close to the centromere of (acrocentric) AK2. (*C* and *D*) The presumed origin of *A. thaliana* chromosomes AT2 to -5. (*C*) Chromosome AT3 has originated because of a reciprocal translocation between AK3 and AK5. The fusion chromosome AT2 arose by means of a translocation between AK3/5 and an acrocentric AK4. A paracentric (Ipa) and a pericentric (Ipe) inversion within AK4 are presumed to explain the origin of AT2. (*D*) AT4 was formed by means of a reciprocal translocation between AK6 and AK7 and subsequent pericentric inversion; additionally, it gained an NOR. Shown is pericentric inversion of AK8 into an acrocentric and subsequent translocation with the short arm of AK6/7 generated AT5. The minichromosomes arising as a second translocation product in *B–D* are dispensable and got lost. The ancestral chromosomes are presumed to bear NORs (empty spheres) at the same positions as in *A. lyrata*; NORs actually found in *A. thaliana* are depicted as black spheres. Inversions (I), translocations (T), and fusions (F) are enumerated as in Fig. 1.

sponding to LG 8 revealed an acrocentric chromosome with a short arm apparently consisting of 45S rDNA (Fig. 3*A6*). The probes corresponding to LGs 4 and 5 each labeled one arm of the same chromosome (Fig. 3*A4*). FISH with differently labeled BAC pools of LGs 4 and 5 revealed a presumably pericentric inversion within AK4, rendering it acrocentric before a reciprocal translocation that fused both LGs and generated a dispensable minichromosome consisting mainly of a centromere and telomeric sequences (Fig. 3*A2*). Because we could not detect an inversion within AK5, a paracentric inversion comprising its short arm, before a pericentric inversion, could have generated an acrocentric AK5 (without interrupting colinearity to LG5) that fused with modified AK4 (Fig. 3*A2*), resembling the fusion of AK3 and AK4 to AT2 (Fig. 2*C*).

In *T. glabra* ($n = 6$), probes designed according to the LGs 1, 4, 6, and 7 each labeled an individual pachytene bivalent (Figs. 3*B1* and 4). The probes for LGs 2 and 8 painted a single chromosome (AK2/8). This chromosome with a centromere within the part derived from AK2 apparently resulted from a pericentric inversion rendering AK8 acrocentric, followed by a reciprocal translocation between AK2 and the acrocentric AK8 (data not shown). The small dispensable translocation product became lost. A second fusion chromosome corresponds to AK3 and AK5. It originated (after a pericentric inversion comprising the short arm of AK3) by means of a reciprocal translocation between the AK3 centromere and the short arm end of AK5. As revealed by differential painting of subregions from the short arms of both ancestral chromosomes, a paracentric inversion occurred within the fusion chromosome AK3/5 (Fig. 3*B2*). Furthermore, differential painting revealed a paracentric inversion in the bottom (long) arm of the chromosome corresponding to AK7 (Fig. 4).

In *H. alpina* ($n = 6$), probes designed according to the LGs 1, 3, 4, and 7 each labeled one individual pachytene bivalent. Apparently, AK8 became acrocentric by means of a pericentric inversion before a reciprocal translocation led to fusion with AK6. A pericentric and subsequently a paracentric inversion happened later on within the long arm of the fusion chromosome involving regions derived from both ancestral chromosomes (Fig. 3*C2*). AK2 and AK5 are combined by translocation of one arm of AK5 to one end and of the second arm of AK5 to the other end of AK2 (Fig. 3*C1* and Fig. 5, which is published as supporting information on the PNAS web site).

The Phylogenetic Tree Indicates Recurrent Chromosome Number Reduction from an Ancestral Karyotype with Eight Chromosome Pairs. Phylogenetic analysis of four independent gene loci supported a largely congruent phylogeny. To visualize the extent of this compatibility between gene trees, the four gene trees were combined into a single supernetwork by using the z-closure rule (ref. 15, Fig. 4, and Fig. 6, which is published as supporting information on the PNAS web site). The inferred phylogenetic relationships resemble those published previously (10, 16), with *H. alpina* being most distantly related to *A. thaliana*. The similar karyotypes of *Arabidopsis* and *Capsella* lineages support the view that the *A. lyrata*/*Capsella* karyotypes resemble the hypothetical ancestral karyotype with eight chromosome pairs. Our data imply that the putative ancestral karyotype ($n = 8$) is older than the split between the *Hornungia* and the *Arabidopsis-Capsella-Turritis* clades. Furthermore, placing reconstructed karyotypes onto the phylogenetic tree suggests that chromosome number reduction was an independent and recurrent process in each of the four lineages analyzed, mostly including different ancestral chromosomes (Fig. 4).

Discussion

Multicolor chromosome painting of pachytene chromosomes of *A. thaliana* with probes arranged according to the linkage groups of *A. lyrata* and *C. rubella* (considered to represent largely the ancestral karyotype of *A. thaliana* and its relatives) have allowed us to detect all inversion, translocation, and fusion events that apparently contributed to the evolution of the *A. thaliana* karyotype, as inferred from comparative genetic maps (7–9, 11). More importantly, chromosome painting using a contiguous BAC tiling path for *A. thaliana* allowed us to localize the centromeres and border chromosomal inversions and translocations more precisely than what was deducible from comparative maps with a low or medium marker density. For the following events, the chronological order of chromosome rearrangements

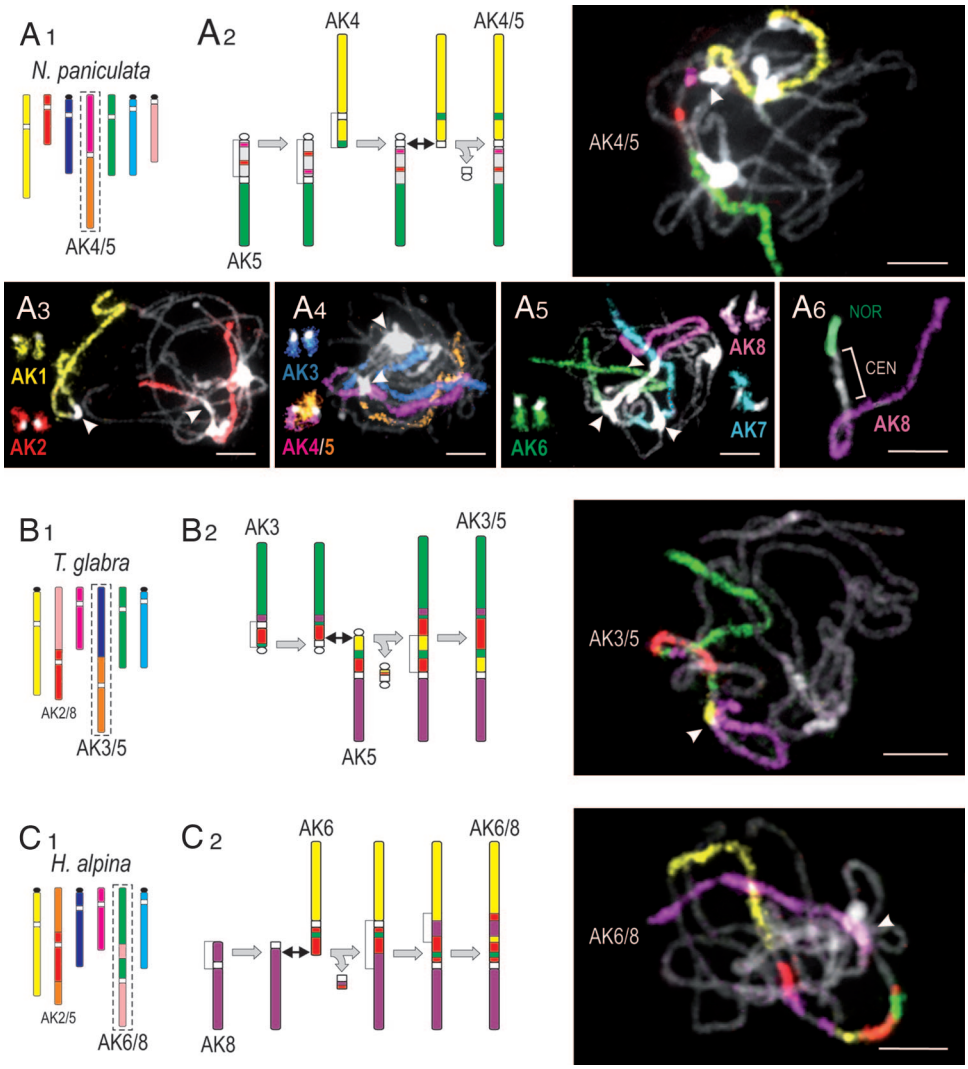

Fig. 3. Idiograms and painted chromosomes of *N. paniculata* ($n = 7$), *T. glabra* ($n = 6$), and *H. alpina* ($n = 6$). Chromosomes are colored according to their colinearity to the ancestral karyotype (AK1 to -8; see Fig. 1) in *A1*, *A3–A5*, and *B1* and *C1*, or according to the differently labeled BAC subcontigs used in CCP (*A2–C2*). (*A3–A5*) CCP in *N. paniculata* performed with *A. thaliana* probes arranged according to the AK1 to -8 chromosomes of *A. lyrata*. Pairs of painted mitotic chromosomes are inserted in *A3–A5*. The presumed origin of the fusion chromosome AK4/5 and painting of this chromosome are shown in *A2*. (*A6*) The probe corresponding to chromosome AK8 labels the long arm of a chromosome that on the other side of the heterochromatic pericentromere region displays only 45S rDNA (green) and thus represents a nearly acrocentric homeolog of AK8. (*B1* and *C1*) Idiograms of reconstructed karyotypes of *T. glabra* (*B1*) and *H. alpina* (*C1*). (*B2* and *C2*) The presumed origin and corresponding painting of the *T. glabra* fusion chromosome AK3/5 (*B2*) and the *H. alpina* fusion chromosome AK6/8 (*C2*). Empty squares/arrowheads indicate centromeric regions, black spheres represent actual NORs, and empty spheres hypothetical NORs (see Fig. 2). (Scale bars: 5 μm.)

leading to chromosome number reduction in *A. thaliana* is fixed (Figs. 1 *A* and *C* and 2 and ref. 11): inversion 1 → fusion 3, resulting in AT1; translocation 1 → inversion 2 (and 3) → fusion 1 resulting in AT4 and AT5; and translocation 2 → para- and pericentric inversions in AK4 → fusion 2, resulting in AT2 and AT3. However, it remains uncertain which group of linked events occurred earlier or later. It is also not clear whether AK8 was originally an acrocentric as in *N. paniculata* where the short arm apparently consists only of 45S rDNA (Fig. 3*A6*) or a submetacentric as in *A. lyrata* and *C. rubella*, before participating in the fusions toward the karyotypes of *A. thaliana*, *T. glabra*, and *H. alpina*. Both assumptions imply repeated pericentric inversions within AK8.

Furthermore, our study suggests that fusion events reducing the basic chromosome number from eight to five are based on reciprocal translocations between meta-/submetacentric and acrocentric chromosomes, the latter generated by pericentric inversions. The minichromosomes that, in addition to the "fusion chromosomes," resulted from these translocation events have presumably been lost. This scenario explains the elimination of centromeres toward the *A. thaliana* karyotype as well as a potential loss of terminal NORs.

An important finding in our study was that CCP reliably detected chromosomal colinearity between *A. thaliana* and more distantly related species for which (comparative) genetic maps are not available (Figs. 3 and 4). CCP has enabled us to elucidate chromosome rearrangements and reductions that have led to present day karyotypes. Our investigation of three such species revealed mainly the same mechanisms to be responsible for chromosome number reduction as found for *A. thaliana*. Remarkably, of the 52 breakpoints contributing to the 26 rearrangements considered in our work, 84.6% involved centromeric (24 breakpoints) or terminal (20 breakpoints) positions where repetitive sequences are clustered. Concordant with our obser-

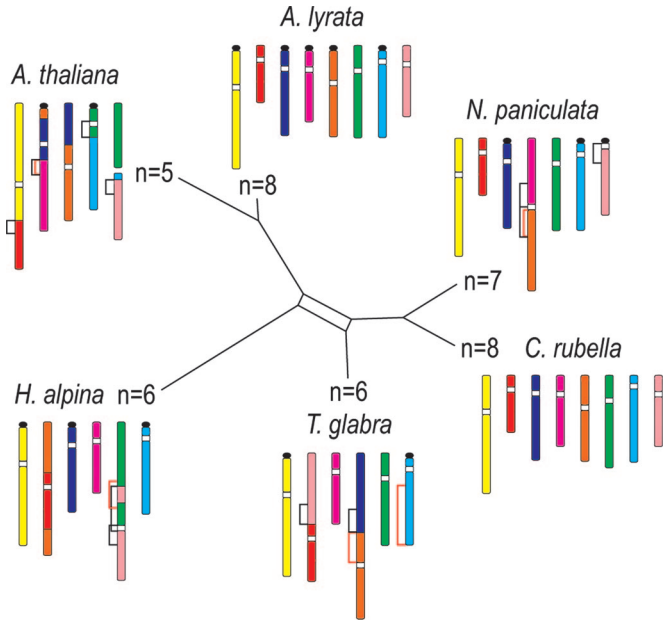

Fig. 4. Idiograms and Supernetwork for the five investigated species and for *C. rubella*. Length of edges in the network is related to evolutionary distance (29). Note that *Capsella bursa-pastoris* gene sequences were used to infer the phylogenetic position of *C. rubella*. *A. lyrata* and *C. rubella* chromosomes are assumed to resemble the ancestral karyotype (AK1 to -8). Colinear chromosomes/chromosome regions are depicted in the same color. Red and black brackets indicate paracentric and pericentric inversions, respectively.

vations, in telomerase-deficient *A. thaliana* plants terminal NORs participate in chromosome rearrangements ≈10 times more often than expected at random (17).

In general, chromosome rearrangements exhibit a low level of homoplasy because the same chromosomal patterns are unlikely to occur independently in different phylogenetic lineages. When shared by different species, such rearrangements represent "rare genomic changes" (18) indicative of phylogenetic relatedness and common ancestry. Ancestral chromosome patterns shared by *H. alpina* and the remaining species support the assumption of a common ancestor for the whole species group. Thus, chromosomal colinearity has an immense potential to infer phylogenetic relationship and/or to refine sequence-based phylogenetic frameworks. Because CCP was successfully adapted also to species of the tribe Brassiceae (19), it should be applicable to clarify chromosome evolution even for taxa of the Brassicaceae family remotely related to *A. thaliana*.

Materials and Methods

Chromosome Preparation. Chromosome spreads were prepared from: *A. thaliana* (accessions Columbia and C24), *A. lyrata* subsp. *lyrata* (Bash Bish, MA; cf. 14), *H.* (*Pritzelago*) *alpina* (Austrian Alps Mountains, Alpengarten Rannach, Austria), *N. paniculata* (Botanic Garden, Copenhagen, Denmark; code no. 28, index no. 783, 2001) and *T.* (*Arabis*) *glabra* (Stangerode, Harz Mountains, Germany). See Table 1, which is published as supporting information on the PNAS web site, for detailed information on species used in this study. Whole inflorescences were harvested from plants grown in a greenhouse, fixed in 6:3:1 ethanol:chloroform:acetic acid overnight and stored in 70% ethanol at −20°C until use. Selected inflorescences were rinsed in distilled water and citric buffer (10 mM sodium citrate, pH 4.8). Flower buds of suitable size were excised and digested in 0.3% pectolyase, cellulase, and cytohelicase (all Sigma) in citric buffer at 37°C for 3–5 h, transferred into citric buffer, and kept at 4°C until use. Individual flower buds were put on a clean slide under a stereomicroscope and disintegrated by a needle in a drop of citric buffer. Subsequently, 10 μl of 45% acetic acid was added to the suspension, and the drop was stirred by a needle on a hot plate (50°C) for 0.5–2 min. During the stirring, 10–40 μl of 45% acetic acid was added. Subsequently, chromosomes were fixed by adding 100–200 μl of ethanol:acetic acid (3:1). The slide was tilted to remove the fixative, dried by a hair dryer, and inspected under phase contrast. Suitable slides were postfixed in 4% formaldehyde dissolved in distilled water for at least 10 min and air-dried.

Probe Labeling, FISH, and Image Processing. The BAC clones used for FISH were obtained from the Arabidopsis Biological Resource Center (Columbus, OH). Isolation of BAC DNA and selection of chromosome-specific clones suitable for chromosome painting was performed as described (14, 20). Table 2, which is published as supporting information on the PNAS web site, shows BAC contigs used for CCP in Figs. 1–3; the detailed list of BACs used for chromosome painting is available upon request. The BAC clone T15P10 (AF167571) bearing 45S rRNA genes was used for *in situ* localization of NORs. For comparative painting, pools of BAC contigs were arranged according the comparative genetic maps between *A. thaliana*/*C. rubella* (9), *A. thaliana*/*A. lyrata* subsp. *petraea* (7), or *A. thaliana*/*A. lyrata* subsp. *lyrata* (8). The designation of LGs and chromosomes of *A. lyrata*, *C. rubella*, and the putative AK was as in Kuittinen *et al.* (7) and Koch and Kiefer (11). Thus, chromosomes AK1 to AK8 correspond to LG 1 to 8 of *A. lyrata* (7) and A to H of *C. rubella* (9), respectively. BAC DNA was labeled by nick translation (21) with biotin-dUTP, digoxigenin-dUTP, dinitrophenyl (DNP)-dUTP, or with Cy3-dUTP (20). For chromosome painting, labeled BACs were pooled, precipitated, and resuspended in 20–40 μl of hybridization mix [20% or 50% (*A. thaliana*) formamide, 10% dextran sulfate, 2× SSC, 50 mM sodium phosphate (pH 7.0)] per slide. Labeled probe and chromosomes were denatured together on a heat block at 80°C for 2 min and incubated in a moist chamber at 37°C for 36–60 h. Posthybridization washing was performed in 50% formamide (*A. thaliana*) or 20% formamide (all other species) in 2× SSC at 42°C. Fluorescent detection was as follows: biotin-dUTP was detected by avidin conjugated with Texas Red (Vector Laboratories), goat anti-avidin conjugated with biotin (Vector Laboratories), and again with avidin conjugated with Texas Red; digoxigenin-dUTP by mouse anti-digoxigenin (Roche Applied Science, Mannheim, Germany) and goat anti-mouse conjugated with Alexa Fluor 488 (Molecular Probes); and DNP-dUTP by rabbit anti-DNP (Sigma) and goat anti-rabbit conjugated with Cy5 (Jackson ImmunoResearch). Cy3-dUTP was observed directly. Chromosomes were counterstained with 2 μg/ml DAPI in Vectashield (Vector Laboratories). Fluorescence signals were analyzed with an Axioplan 2 epifluorescence microscope (Zeiss) by using ×100/1.4 Zeiss plan apochromat objective and cooled charge-coupled device (CCD) camera (Spot 2e, Diagnostic Instruments, Sterling Heights, MI). Images were acquired separately for all five fluorochromes by using the appropriate excitation and emission filters (AHF Analysentechnik, Lagenfeld, Germany). The five monochromatic images were pseudocolored and merged by using ADOBE PHOTOSHOP 6.0 software (Adobe Systems, San Jose, CA). Eight pseudocolors were applied to depict the eight linkage groups/chromosomes of an ancestral karyotype.

DNA-Based Phylogenetic Reconstruction. Nucleotide sequences of five genes were obtained for each of the taxa genetically mapped and/or analyzed by CCP, as well as for the taxa *Boechera stricta*, *Camelina microcarpa*, *Crucihimalaya wallichii*, *Lepidium apetalum*, *Olimarabidopsis pumila*, *Pachycladon novae-zelandiae* and

Physaria gracilis. Phylogenetic analysis of these genes was undertaken to help evaluate an unrooted species phylogeny for these species. *A. thaliana* sequences were obtained from GenBank (accession nos. M64119, AY198405, X52320, and AP000423). All sequences unique to this study have been deposited in GenBank (accession nos. DQ310510-DQ310545). Genomic DNA was isolated from leaves by using the plant Dneasy minikit (Qiagen, Valencia, CA). Five genes were PCR amplified and sequenced: (*i*) the single copy gene encoding cytosolic glyceraldehyde-3-phosphate dehydrogenase (*G3Pdh*) (22); (*ii*) the single copy gene encoding *FRIGIDA* (*FRI*) (23); (*iii*) the multicopy internal transcribed spacer (ITS), including ITS1, 5.8S, and ITS2 of the nuclear ribosomal DNA sequence units (24); and (*iv* and *v*) the two chloroplast loci, ribulose-1,5-bisphosphate carboxylase/oxygenase large subunit gene (*rbc*L, 25) and *trn*L–*trn*F spacer (26). Because both *rbc*L and the *trn*L-*trn*F regions potentially evolve as a unit, we concatenated these as a single CpDNA marker.

Sequence contigs were prepared by using SEQUENCHER 4.2 (Gene Codes, Ann Arbor, MI), and visually aligned with MACCLADE 4.06 (27) by using the *A. thaliana* gene structure and sequence as a reference. Gene trees were estimated by maximum likelihood (ML) by using PAUP 4.0 [options: exhaustive search; Multrees (save multiple trees), and TBR (tree bisection and reconnection) branch swapping]. Substitution models were selected by MODELTEST 3.5 (28) under the Akaike information criterion, with parameters estimated during ML exhaustive searches. It was necessary to constrain *Hornungia*, *Lepidium*, and *Physaria* to a monophyletic group in the ITS tree. These four trees have been combined by using the Z-closure super network procedure (15), as implemented in SPLITSTREE 4.1 (29).

We thank J. Bruder, M. Kühne, and R. Schubert for technical assistance and P. Lockhart and R. Rieger for critical reading of the manuscript. This work was supported in part by a grant from the German Research Foundation (DFG) (to M.A.L. and I.S.). The Allan Wilson Centre is acknowledged for supporting K.M. during this study.

1. Schubert, I., Rieger, R. & Künzel, G. (1991) in *Chromosome Engineering in Plants: Genetics, Breeding, Evolution (Part A)*, eds. Gupta, P. K. & Tsuchiya, T. (Elsevier, Amsterdam), pp. 113–140.
2. Schubert, I. & Rieger, R. (1994) in *Chromosomal Alterations: Origin and Significance*, eds. Obe, G. & Natarajan, A. T. (Springer, Berlin), pp. 380–394.
3. Moore, G., Devos, K. M., Wang, Z. & Gale, M. D. (1995) *Curr. Biol.* **5,** 737–739.
4. Wienberg, J. (2004) *Curr. Opin. Genet. Dev.* **14,** 657–666.
5. Murphy, W. J., Pevzner, P. A. & O'Brien, S. J. (2004) *Trends Genet.* **20,** 631–639.
6. Appel, O. & Al-Shehbaz, I. A. (2003) in *The Families and Genera of Vascular Plants*, eds. Kubitzki, K. & Bayer, C. (Springer, Berlin), Vol. 5, pp. 75–174.
7. Kuittinen, H., de Haan, A. A., Vogl, C., Oikarinen, S., Leppälä, J., Koch, M., Mitchel-Olds, T., Langley, C. H. & Savolainen, O. (2004) *Genetics* **168,** 1575–1584.
8. Yogeeswaran, K., Frary, A., York, T. L., Amenta, A., Lesser, A. H., Nasrallah, J. B., Tanksley, S. D. & Nasrallah, M. E. (2005) *Genome Res.* **15,** 505–515.
9. Boivin, K., Acarkan, A., Mbulu, R. S., Clarenz, O. & Schmidt, R. (2004) *Plant Physiol.* **135,** 735–744.
10. Koch, M., Bishop, J. & Mitchell-Olds, T. (1999) *Plant Biol.* **1,** 529–537.
11. Koch, M. A. & Kiefer, M. (2005) *Am. J. Bot.* **92,** 761–767.
12. Hansson, B., Kawabe, A., Preuss, S., Kuittinen, H. & Charlesworth, D. (2006) *Genet. Res.*, in press.
13. The Arabidopsis Genome Initiative (2000) *Nature* **408,** 796–815.
14. Lysak, M. A., Pecinka, A. & Schubert, I. (2003) *Chromosome Res.* **11,** 195–204.
15. Huson, D. H., Dezulian, T., Kloepper, T. & Steel, M. A. (2004) *Lect. Notes Comput. Sci.* **3240,** 388–399.
16. Koch, M., Haubold, B. & Mitchell-Olds, T. (2001) *Am. J. Bot.* **88,** 534–544.
17. Siroky, J., Zluvova, J., Riha, K., Shippen, D. E. & Vyskot, B. (2003) *Chromosoma* **112,** 116–123.
18. Rokas, A. & Holland, P. W. H. (2000) *Trends Ecol. Evol.* **15,** 454–459.
19. Lysak, M. A., Koch, M. A., Pecinka, A. & Schubert, I. (2005) *Genome Res.* **15,** 516–525.
20. Pecinka, A., Schubert, V., Meister, A., Kreth, G., Klatte, M., Lysak, M. A., Fuchs, J. & Schubert, I. (2004) *Chromosoma* **113,** 258–269.
21. Ward, P. B. (2002) in *FISH: A Practical Approach*, Practical Approach Series, eds. Beatty, B., Mai, S. & Squire, J. (Oxford Univ. Press, Oxford), Vol. 260, pp. 5–28.
22. Strand, A. E., Leebens-Mack, J. & Milligan, B. G. (1997) *Mol. Ecol.* **6,** 113–118.
23. Le Corre, V., Roux, F. & Reboud, X. (2002) *Mol. Biol. Evol.* **19,** 1261–1271.
24. White, T. J., Bruns, T., Lee, S.& Taylor, J. (1990) in *PCR Protocols: A Guide to Methods and Applications*, eds. Innis, M. A., Gelfand, D. H., Snisky, J. J. & White, T. J. (Academic, San Diego), pp. 315–322.
25. Chase, M. W., Soltis, D. E., Olmstead, R. G., Morgan, D., Les, D. H., Mishler, B. D., Duvall, M. R., Price, R. A., Hills, H. G., Qiu, Y.-L., *et al.* (1993) *Ann. Missouri Bot. Garden* **80,** 528–580.
26. Taberlet, P., Gielly, L., Pautou, G. & Bouvet, J. (1991) *Plant Mol. Biol.* **17,** 1105–1109.
27. Maddison, D. R. & Maddison, W. P. (2000) MACCLADE 4: *Analysis of Phylogeny and Character Evolution* (Sinauer, Sunderland, MA).
28. Posada, D. & Crandall, K. A. (1998) *Bioinformatics* **14,** 817–818.
29. Huson, D. H. & Bryant, D. (2006) *Mol. Biol. Evol.* **23,** 254–267.